Published in IET Communications
Received on 3rd July 2013
Revised on 25th April 2014
Accepted on 15th June 2014
doi: 10.1049/iet-com.2014.0046

ISSN 1751-8628

Error probability performance analysis for multicarrier direct sequence code division multiple access multiple-input–multiple-output systems over correlated η–μ fading channels

James Osuru Mark Amok, Naufal Mohamed Saad

Department of Electrical and Electronics Engineering, Universiti Teknologi PETRONAS, 31750 Bandar Seri Skandar, Tronoh, Perak, Malaysia
E-mail: osuruamok@gmail.com

Abstract: The authors investigate the performance of multiple-input–multiple-output multicarrier direct sequence code division multiple access system operating over arbitrarily and equally correlated η–μ fading channels in terms of average bit error probability and average symbol error probability. Closed form expressions for average error probability using moment generating function-based approach are derived and expressed in terms of Lauricella's multivariate hypergeometric functions. Furthermore, based on numerical results, they observe that the performance of the system improves when the number of multipath clusters increases as well as the number of subcarriers (frequency diversity). Similarly, substantial enhancement in system performance is observed due to the effect of spatial diversity. Finally, they verify the results via Monte Carlo simulation-based method to support the accuracy of the analytical approach and also compare with already published ones.

1 Introduction

In wireless communication systems, deployment of multiple antennas at both the transmitter and receiver side improves the channel capacity and decreases the average error probability of the received signal as well. Furthermore, the system performance is enhanced if the spacing between two adjacent antennas is not too close to yield correlation between the spectra of the received signals. In practice, the effect of correlation on the spectra of the received signal exist but can only be minimised by setting an appropriate spacing between the adjacent antennas of the wireless communication system.

The incorporation of multiple antennas into the broadband wireless communication systems such as multicarrier direct sequence code division multiple access (MC DS CDMA) system will increase the channel capacity and reduce the effect of multipath fading [1]. MC DS CDMA system is a wireless communication system that is formed out of the combination of direct sequence code division multiple access (DS CDMA) and orthogonal frequency division multiplexing [2]. This system inherits the advantages and disadvantages of its constituents. The operation of MC DS CDMA system in this particular case is based on time domain but in other situations it can use both time domain and frequency domain, respectively. In addition, the transmitted data is first serial to parallel converted, each data is assigned a spreading code and mapped to a number of subcarriers. Therefore the signals are combined and then transmitted. Furthermore, the signal modulation and demodulation is carried out with the aid of inverse fast Fourier transform (IFFT) and fast Fourier transform (FFT) and DS CDMA assigns code to each signal [1]. Owing to the application of multiple-input–multiple-output (MIMO) systems to both sides of MC DS CDMA systems, specifically at the receiving terminal, the envelopes of the transmitted signals are likely to become correlated if the spacing between adjacent antennas is not placed well to avoid correlation. In this case, extensive research has been done on this as supported by the publications outlined below.

In [3], the operation of an interleaved MC CDMA system with MRC receiver over correlated Nakagami-m fading channels was investigated in terms of bit error rate. The authors employed probability density function (PDF)-based approach to obtain the average bit error probability (ABEP). Feng and Qin [4] explored the performance of MC CDMA system with MRC diversity operating over correlated Nakagami-m fading channels in terms of ABEP. The closed form expressions for average error probability were determined using moment generating function (MGF)-based approach. The authors in [5] examined the performance of MC CDMA system with equal gain combining diversity technique working over correlated Nakagami-m fading channels in terms of ABEP. They utilised expansion in central difference method to calculate the ABEP of the system. The operation of space-time block code (STBC) MC CDMA system over independent and correlated fading channels in likelihood receiver and linear receiver was

investigated [6]. The authors employed bit error rate as a metric for performance evaluation. Xu and Milstein [7] proposed a wireless communication system (multicarrier) that reduces the effect of correlation among the subcarriers, suppresses partial band interference and operates over frequency selective Rayleigh fading channels. They used ABEP to measure the performance of the system. In [8], Elnoubi and Hashem explored the performance of MC DS CDMA MIMO system with radio activated key entry (RAKE) receiver operating over correlated Nakagami-*m* fading channels in terms of ABEP. The authors used numerical technique to evaluate the ABEP performance of the system. The performance of cyclic diversity and STBC MC CDMA system working over correlated Nakagami-*m* fading channels in terms of average symbol error probability (ASEP) was investigated in [9]. In this case, the subcarriers of the system are considered to be correlated. The closed form expressions for ASEP were obtained using MGF-based approach and expressed in Gauss hypergeometric and Appell's hypergeometric functions, respectively. Yang [10] studied the bit error rate performance of the multiantenna MC DS CDMA system over correlated time selective Rayleigh fading channels. The space-time spreading technique based on the family of orthogonal variable spreading factor code was proposed in order to attain time diversity. He examined the performance of multiantenna MC DS CDMA system operating over correlated time selective Rayleigh fading channels in terms of ABEP. The investigation and analysis of the performance of MRC MC CDMA system based on minimum shift keying modulation technique over independent and correlated Nakagami-*m* and Rician fading channels in terms of ABEP was carried out in [11]. In addition, the effect of frequency offset was also considered. Asghari *et al.* [12] explored the performance of the system based on rectangular quadrature amplitude modulation (QAM) modulation scheme over correlated η–μ fading channels in terms of ASEP. The exact closed form expressions for ASEP were determined using MGF-based approach and expressed in Lauricella's multivariate hypergeometric functions. In [13], Subadar and Shu examined the operation of an L-branch maximum ratio combining receiver system over equally correlated η–μ fading channels in terms of ABEP and outage probability. The effect of MIMO systems on the performance of MC DS CDMA system operating over independent identically distributed (i.i.d) η–μ flat fading channels in terms of average channel capacity and average error probability was investigated in [14].

As we observe from the samples of the empirical literature review outlined above, the fading distributions utilised to study the performance of MC DS CDMA systems working over correlated fading channels are Rayleigh, Rician, Nakagami-*m* and so forth but not including η–μ fading distribution. In this paper, we examine the performance of MC DS CDMA MIMO system operating over arbitrarily and equally correlated η–μ fading channels in terms of ABEP and ASEP, respectively. Closed form expressions for average error probability are determined using MGF-based approach. These expressions are expressed in Lauricella's multivariate hypergeometric functions. The derived formulas are new.

The organisation of the remaining parts of this paper is as follows. Section 2 describes the system and channel models, respectively. In Section 3, derivation of MGF of the instantaneous signal-plus-interference-noise ratio (SINR) is carried out. In Section 4, the ABEP and ASEP for the system operating over arbitrarily and equally correlated η–μ fading channels are developed. Numerical examples illustrating graphically the performance of the system and discussions are presented in Section 5. Section 6 concludes the paper.

2 System and channel model description

In this section, we assume that MC DS CDMA MIMO system has M_t number of transmit antennas and N_r number of receive antennas, respectively. Then, the channel between the transmit antenna and the receive antenna pair is assumed to be quasi-static with flat fading conditions. Similarly, we presume the system operation depends on channel state information available at the receiver, meanwhile the transmitter employs STBC for the receiver to gain transmit diversity. In this case, orthogonal MC DS CDMA system is utilised to represent the class of MC DS CDMA system we are examining in this work [1]. Thus, the input data is first serial to parallel converted to substreams. Therefore the symbol in each substream is spread in time domain and then mapped to each subcarrier and M_t transmit antennas, respectively. Hence, in each subcarrier, each signal is modulated by invoking IFFT. In this way, the modulated signals are all added together and transmitted. In addition, we assume that the subcarriers are correlated if the separation between two adjacent subcarriers is less that $1/T_c$, where T_c is the chip duration of the orthogonal spreading code. Consequently, the envelopes of the received signals will experience correlation which reduces the quality of the signal at the receiving end. In this situation, we presume that the transmitter has two antennas while the receiver has N_r antennas. We also consider two symbols $S_1^k(t)$ and $S_1^k(t)$ to be transmitted simultaneously using Alamouti-based approach. Thus, $S_1^k(t)$ symbol is transmitted from antenna 1 and $S_2^k(t)$ symbol is also transmitted from antenna 2 simultaneously at the first time slot. Meanwhile, the complex conjugate of $-S_2^k(t)$ is transmitted from antenna 1 and also the complex conjugate of $S_1^k(t)$ is transmitted from antenna 2 simultaneously at the second time slot. Hence, the condition of the channel between the transmitter and receiver antennas pair is assumed to be frequency non-selective fading. Therefore the transmitted signals by user k can be expressed as [1]

$$\begin{aligned} S_1^k(t) &= \sum_{i=1}^{q}\sum_{j=1}^{U}\sqrt{\frac{2P}{M_t U}}c_1^k(t)b_{1,i,j}^k(t)\cos\left(2\pi f_{ij}t+\varphi_{ij}^1\right) \\ S_2^k(t) &= \sum_{i=1}^{q}\sum_{j=1}^{U}\sqrt{\frac{2P}{M_t U}}c_2^k(t)b_{2,i,j}^k(t)\cos\left(2\pi f_{ij}t+\varphi_{ij}^2\right) \end{aligned} \tag{1}$$

where $b_{1,i,j}^k(t)$ and $b_{2,i,j}^k(t)$ are described as odd and even data stream transmitted by user k and represented by the expression

$$b^k(t)=\sum_{n=-\infty}^{\infty}b^k[n]P_{T_s}(t-nT_s) \tag{2}$$

where $b^k[n]\in(+1,\ -1)$ represents binary data sequence modulating uth subcarriers, T_s is the symbol duration, $P_{T_s}(t)$ is a rectangular pulse uniformly distributed in interval $[0,\ T_s)$. $c_1^k(t)$ and $c_2^k(t)$ denote spreading codes in time domain for transmitter 1 and 2, respectively. The spreading

doi: 10.1049/iet-com.2014.0046

code is expressed as

$$c^k(t) = \sum_{n=-\infty}^{\infty} c^k[n]\psi(t - nT_c) \tag{3}$$

where T_c is the chip duration, $c^k[n] \in (+1, -1)$ with equal probability and $\psi(t)$ is a rectangular chip waveform in time domain over the interval $[0, T_c)$. U is the number of subcarriers, q is the number of bits in the data stream, then this data stream is converted from serial to parallel to the q number of lower rate substreams where each is assigned a time domain spreading code $c(t)$ and is then transmitted by a number of subcarriers to attain frequency diversity. P is the transmitted power, f_{ij} is the subcarrier frequency of the ith bit at jth subcarrier and ϕ_{ij} is the phase introduced by the multicarrier modulation. Specifically, the characteristics of the channel do not change during one time slot or symbol frame but can change after another interval of time or another symbol frame. Since we are considering two symbols to be transmitted using two transmit antennas using Alamouti-based approach, the code rate for STBC is one. Therefore the extension of the number of transmit antennas from 2 upwards may also lead to the consideration of the effects of other code rates for STBC such as 0.5 and 0.75, respectively.

In case of the channel existing between M_t transmit antennas and N_r receive antennas, we assume that it is frequency non-selective fading and the subcarriers of the system are correlated. So the received signal envelope is modelled as η–μ fading distribution [15]. Furthermore, the impulse response for user k transmitting data over jth subcarriers is given by

$$h_j^k(t) = \alpha_j^k \delta(t - \tau_k) \exp(-i\psi_j^k) \tag{4}$$

where α is an attenuation factor, τ is the delay, $\delta(.)$ is the Kronecker delta function and ψ is the phase shift. Generally, α, τ and ψ are assumed to be constant over two symbols interval. Furthermore, τ_k for kth data is presumed to be uniformly distributed over $[0, T_s)$ interval. Now we can revisit η–μ fading distribution. The η–μ fading distribution is a generalised distribution that models short term signal envelope variation in a non-line of sight condition [15]. It includes Nakagami-q and Nakagami-m distribution as particular cases. In this case, the received signal comprises of cluster of multipath waves propagating in a non-homogeneous environment. Hence, the in-phase and quadrature components of the fading signal envelope within each cluster are assumed to be independent of each other and have different powers (format 1). Then, η is the scattered power ratio between the in-phase and quadrature components of each cluster of the multipath. Therefore, the parameters h and H are expressed as a function of η, $h = (2 + \eta + \eta^{-1})/4$ and $H = (\eta^{-1} - \eta)/4$, $0 < \eta < \infty$ for format 1 [16]. On the other hand, the in-phase and quadrature components within each cluster are assumed to have the same powers and correlated with each other. Then, the parameters h and H are expressed in terms of η fading parameter as $h = 1/(1 - \eta^2)$ and $H = \eta/(1 - \eta^2)$, $-1 < \eta < 1$ for format 2. Therefore the PDF of η–μ fading distribution for both formats (1 and 2) in terms of envelope power is given by [15]

$$f(\gamma) = \frac{2\sqrt{\pi}\mu^{\mu+0.5}h^{\mu}}{\Gamma(\mu)H^{\mu-0.5}\overline{\gamma}^{\mu+0.5}}\gamma^{\mu-0.5}\exp\left(-\frac{2\mu h\gamma}{\overline{\gamma}}\right)I_{\mu-0.5}\left(\frac{2\mu H\gamma}{\overline{\gamma}}\right) \tag{5}$$

where $\mu = (E^2(\alpha^2)/2\mathrm{Var}(\alpha^2))(1 + (H/h)^2)$, $\mu > 0$ is the number of multipath clusters, $\Gamma(.)$ is the Gamma function defined as $\int_0^{\infty} t^{x-1}e^{-t}\,dt$, $I_x(.)$ is the modified Bessel function of the first kind and order x, $\overline{\gamma}$ is the average signal-to-noise ratio (SNR), $E(.)$ and $\mathrm{Var}(.)$ represent expectation and variance operators and α is the signal envelope. In case of details regarding η–μ distribution see [15].

The orthogonal MC DS CDMA MIMO system is considered to support K asynchronous active users communicating with the base station within a single cell. Here, the number of subcarriers is the same as that of the spreading factor ($N_e = T_s/T_c$), with the subcarriers being correlated. Thus, the average power received from each user at the base station is assumed to be the same. Therefore the received signal is demodulated using FFT-based multicarrier demodulation so as to obtain U number of parallel stream similar to that transmitted [1]. So each data stream is dispread to form a decision variable for each data bit transmitted. For that reason, combining and detection of the received data is performed and then parallel to serial conversion is carried out to produce the original data at the output. Hence, the received signal in the first time slot interval is as in [17] (see (6))

Similarly, the received signal in the second time slot is (see (7))

where K represents the number of active users, n is the nth number of the N_r receive antennas, h_{j1} and h_{j2} are channel impulse response for transmitter 1 and 2 respectively, ϕ_{ij}^1 and ϕ_{ij}^2 are the phases that are introduced during modulation with respect to transmitter 1 and 2 and * denotes complex conjugate. Then, n_1^n and n_2^n denote additive white Gaussian noise (AWGN) modelled as i.i.d complex Gaussian random variables with zero mean and double sided power spectral density of $N_0/2$.

3 Derivation of MGF of instantaneous SINR at the receiver output

The MGF of the instantaneous SINR at the output of the receiver is derived in this section. Basically, we employ (6) and (7) to obtain SINR at the receiver output. The complex conjugate of (7) is first obtained and expresses the results

$$r_1^n(t) = \sum_{k=1}^{K}\sum_{i=1}^{q}\sum_{j=1}^{U}\mathrm{Re}\left(\sqrt{\frac{2P}{M_tU}}\left(c_1^k(t - t_k)b_{1,i,j}^k(t - t_k)h_{j1}e^{j(2\pi f_{ij}t + \varphi_{ij}^1)} + c_2^k(t - t_k)b_{2,i,j}^k(t - t_k)h_{j2}e^{j(2\pi f_{ij}t + \varphi_{ij}^1)}\right)\right) + n_1^n \tag{6}$$

$$r_2^n(t) = \sum_{k=1}^{K}\sum_{i=1}^{q}\sum_{j=1}^{U}\mathrm{Re}\left(\sqrt{\frac{2P}{M_tU}}\left(-c_1^{k*}(t - t_k)b_{2,i,j}^{k*}(t - t_k)h_{j1}e^{-j(2\pi f_{ij}t + \varphi_{ij}^2)} + c_2^{k*}(t - t_k)b_{1,i,j}^{k*}(t - t_k)h_{j2}e^{-j(2\pi f_{ij}t + \varphi_{ij}^1)}\right)\right) + n_2^n \tag{7}$$

with (6) in matrix form. In this case, expressions for the user of interest, multiuser interference because of the same subcarrier frequencies, multiuser interference because of different subcarrier frequencies and noise engendered by AWGN can be determined. Hence, multiuser interference and noise are assumed as Gaussian random variables with zero mean and can be approximated using standard Gaussian approximation method. The detail analysis of the derivation is in [14] and we note the final results as

$$\gamma = \gamma_c \sum_{j=1}^{U} \sum_{m=1}^{M_t} \sum_{n=1}^{N_r} \left| h_{jmn} \right|^2 \tag{8}$$

where h_{jmn} is the channel gain from jth subcarrier, mth transmit antenna to nth receive antenna, γ_c is the total variance, then, $\gamma_{jmn} = \gamma_c |h_{jmn}|^2$, $\overline{\gamma}_{jmn} = \gamma_c E(|h_{jmn}|^2)$ is the average SNR. Therefore we can further expressed the instantaneous SINR as

$$\gamma = \sum_{n=1}^{N_r} \gamma_n = \sum_{n=1}^{N_r} \sum_{m=1}^{M_t} \gamma_{mn} = \sum_{n=1}^{N_r} \sum_{m=1}^{M_t} \sum_{j=1}^{U} \gamma_{jmn} \tag{9}$$

where (9) is a simplified version of (8) in order to be easy to determine the MGF of instantaneous SINR, γ_n, γ_{nm} and γ_{nmj} represent instantaneous SINR on nth receive antenna, mth transmit antenna and jth subcarrier, respectively. Hence, γ_{nmj} models η–μ fading distribution. In this case, we consider the system operating over N_r correlated receive antennas. Suppose $\{X_i\}_{i=1}^{N_r M_t U}$ is a set of $N_r M_t U$ correlated not necessarily identically distributed η–μ elements of the in-phase components of the fading signal envelope with parameters η and μ, respectively. Then, the correlation coefficient between X_i and $X_{i'}$ in-phase components is [18]

$$\rho_{ii'} = \rho_{i'i} = \frac{\operatorname{cov}(X_i, X_{i'})}{\sqrt{\operatorname{Var}(X_i)\operatorname{Var}(X_{i'})}}, \quad 0 \le \rho \le 1 \tag{10}$$

Similarly, $\{Y_i\}_{i=1}^{N_r M_t U}$ is another set of correlated not necessarily identically distributed η–μ elements of the quadrature components of the fading signal envelope with parameters η and μ, respectively. Thus, the correlation coefficient between Y_i and $Y_{i'}$ is the same as in (10) but in terms of Y_i and $Y_{i'}$. Furthermore, the envelope at the output of the receiver is [12] $R^T R = X^T X + Y^T Y$. The MGF of the instantaneous SINR at the output of the receiver is as in Appendix 1 (see (11))

In this case, we consider constant correlation model as a special case, all channels are assumed to have the same average SINR and same fading parameters η and μ [19], that is, constant correlation across all the channels. Consequently, the eigenvalues of the matrices $F_1 = B_{jmn} C^{xx}_{jmn}$ and $F_2 = B_{jmn} D^{yy}_{jmn}$ are given by Alouini *et al.* [18] $\lambda_1^x = \sigma_x^2(1-\rho)$, $\lambda_2^x = \sigma_x^2\big(1 + (N_r M_t U - 1)\rho\big)$, that is, for $N_r M_t U - 1$ fold zero, and for single zero, respectively, for F_1 and similarly for F_2 as $\lambda_1^y = \sigma_y^2(1-\rho)$, $\lambda_2^y = \sigma_y^2\big(1 + (N_r M_t U - 1)\rho\big)$.

In addition, we can now express the MGF of the SINR in terms of eigenvalues expressions [19] (see (12))

On the other hand, in practice, the average SNR in each receiver branches are different, therefore, using the eigenvalues of F_1 and F_2, (11) can be written as

$$\Phi_{x+y}(s) = \prod_{j=1}^{U} \prod_{m=1}^{M_t} \prod_{n=1}^{N_r} \frac{1}{(1 + 2s\lambda^x_{jmn})^{\mu_{imn}} (1 + 2s\lambda^y_{jmn})^{\mu_{jmn}}} \tag{13}$$

Therefore (13) represents a general form of the MGF of instantaneous SINR at the receiver output with arbitrary eigenvalues. Hence, suppose $M_t = 1$, $U = 1$, $K = 1$ and $N_r = V$ in [12], the multiplicities ξ_v^x and ξ_v^y each equal to 2 μ, then, (13) diminishes to [12, Eq. (12)].

4 Average error probability analysis

In this section, we derive the average bit and ASEP of the system using MGF-based approach in order to investigate the system performance. The digital modulation format employed is binary phase shift keying (BPSK), M-ary PSK and square M-ary QAM (MQAM), respectively.

4.1 ABEP of BPSK modulation scheme

Here, we evaluate the ABEP of BPSK digital modulation technique for the system operating over arbitrarily and constant correlated η–μ fading channels. The conditional error probability of coherent BPSK digital modulation technique is given by [20]

$$P_b(\gamma) = Q(\sqrt{2\gamma}) \tag{14}$$

where $Q(x)$ is the Gaussian Q-function. Then, the alternative representation of $Q(x)$ is expressed as [21]

$$Q(x) = \pi^{-1} \int_0^{0.5\pi} \exp\left(-\frac{x^2}{2\sin^2\theta}\right) \mathrm{d}\theta \tag{15}$$

The ABEP of BPSK is given by

$$P_b = \frac{1}{\pi} \int_0^{0.5\pi} \Phi_{x+y}\left(s = \frac{1}{\sin^2\theta}\right) \mathrm{d}\theta \tag{16}$$

Therefore, from (12) and (16), using substitution $t = \cos^2\theta$ and further manipulation, we have the ABEP of BPSK for the system working over equally correlated η–μ fading channels as in Appendix 2 (see (17) on the bottom of the next page)

Furthermore, from (13) and (16), putting $t = \cos^2\theta$ and further manipulation, the ABEP of BPSK for the system operating

$$\Phi_{x+y}(s) = \prod_{n=1}^{N_r} \prod_{m=1}^{M_t} \prod_{j=1}^{U} \frac{1}{\left(\det\left(I_{jmn} + 2sB_{jmn} C^{xx}_{jmn}\right)^{\mu_{jmn}} \det\left(I_{jmn} + 2sB_{jmn} D^{yy}_{jmn}\right)^{\mu_{jmn}}\right)} \tag{11}$$

$$\Phi_{x+y}(s) = (1 + 2s\lambda_1^x)^{-(N_r M_t U - 1)\mu} (1 + 2s\lambda_1^y)^{-(N_r M_t U - 1)\mu} (1 + 2s\lambda_2^x)^{-\mu} (1 + 2s\lambda_2^y)^{-\mu} \tag{12}$$

doi: 10.1049/iet-com.2014.0046

over arbitrarily correlated η–μ fading channels is (see (18))

Suppose $U=1$, $K=1$, $M_t=1$ and $N_r=V$, then, (18) reduces to [12, Eq. (19)].

4.2 ASEP of MPSK digital modulation technique

In this subsection, we determine the ASEP of M-ary PSK modulation scheme for the system working over arbitrarily and equally correlated η–μ fading channels. The conditional error probability of the coherent M-ary PSK digital modulation format is expressed (accurate and approximate) as in [20] and its alternative representation is [21]

$$P_{\mathrm{MPSK}} = \frac{1}{\pi}\int_0^{\pi(1-M^{-1})} \exp\left(-\frac{g_{\mathrm{MPSK}}\gamma}{\sin^2\theta}\right)\mathrm{d}\theta \tag{19}$$

where $g_{\mathrm{MPSK}}=\sin^2(\pi/M)$. Then, the ASEP is

$$P_{s,\mathrm{MPSK}} = \frac{1}{\pi}\int_0^{0.5\pi} \Phi_{x+y}\left(\frac{g_{\mathrm{MPSK}}}{\sin^2\theta}\right)\mathrm{d}\theta + \frac{1}{\pi}\int^{\pi-\pi M^{-1}} \Phi_{x+y}\left(\frac{g_{\mathrm{MPSK}}}{\sin^2\theta}\right)\mathrm{d}\theta \tag{20}$$

Using (12) and (20), then putting $t=\cos^2\theta$ and simplify further, the first integral becomes (see (21))

Analogously, we use the substitution $t=\cos^2\theta/\cos^2(\pi/M)$ and manipulate further, the second integral becomes [22] (see (22))

Therefore the sum of the results of I_1 and I_2 yields that of the ASEP of MPSK digital modulation format for the system operating over equally correlated η–μ fading environment.

In case of arbitrarily correlated η–μ fading channels, we can obtain the ASEP of M-ary PSK digital modulation technique using (13) and (20) yielding (see (23) at the bottom of the next page)

Use substitution $t=\cos^2\theta$ in first integral, employ basic concepts of Algebra and Calculus, we have (see (24) at the bottom of the next page)

Similarly, putting $t=\cos^2\theta/\cos(\pi/M)$ in the second integral, and simplify further, we have (see (25) at the bottom of the next page)

Therefore the summation of I_1 and I_2 yields the ASEP of M-ary PSK scheme for MIMO MC DS CDMA system operating over arbitrarily correlated η–μ fading channels. Since Nakagami-q ($\mu=0.5$, $b=(1-\eta)/(1+\eta)$, $q=\sqrt{\eta}$) is a particular case of η–μ fading distribution, then, suppose $U=1$, $K=1$ and the system operates over i.i.d (correlation coefficient $r=0$) fading environment the summation of I_1 and I_2 reduces to [23, Eq. (10)]. Similarly, when $M_t=1$, $U=1$, $K=1$ and $N_r=L$, that is, to say in case of i.i.d (correlation coefficient $r=0$) fading channels, (24) lessen to [24, Eq. (7)] and (25) diminishes to [24, Eq. (5)]. In addition, since Nakagami-m ($\eta\to 0$, $\eta\to\infty$, $\eta\to\pm 1$)

$$P_b = \frac{\Gamma(2N_rM_tU\mu+0.5)}{2\sqrt{\pi}\Gamma(2N_rM_tU\mu+1)}(1+2\lambda_1^x)^{-\mu(N_rM_tU-1)}(1+2\lambda_1^y)^{-\mu(N_rM_tU-1)}(1+2\lambda_2^x)^{-\mu}(1+2\lambda_2^y)^{-\mu} \times F_D^4\left(0.5,\ \mu\left(N_rM_tU-1\right),\ \mu\left(N_rM_tU-1\right),\ \mu,\ \mu;\ 2N_rM_tU\mu+1;\ \frac{1}{1+2\lambda_1^x},\ \frac{1}{1+2\lambda_1^y},\ \frac{1}{1+2\lambda_2^x},\ \frac{1}{1+2\lambda_2^y}\right) \tag{17}$$

$$P_b = \frac{\Gamma\left(2\sum_{j=1}^{U}\sum_{m=1}^{M_t}\sum_{n=1}^{N_r}\mu_{jmn}+0.5\right)}{2\sqrt{\pi}\Gamma\left(2\sum_{j=1}^{U}\sum_{m=1}^{M_t}\sum_{n=1}^{N_r}\mu_{jmn}+1\right)}\left(\prod_{j=1}^{U}\prod_{m=1}^{M_t}\prod_{n=1}^{N_r}(1+2\lambda_{jmn}^x)^{-\mu_{jmn}}(1+2\lambda_{jmn}^y)^{-\mu_{jmn}}\right) \times F_D^{(2UM_tN_r)}\left(0.5,\ \mu_{111},\ \mu_{112},\ \ldots,\ \mu_{UM_rN_r},\ \mu_{111},\ \mu_{112},\ \ldots,\ \mu_{UM_tN_r};\ 2\sum_{j=1}^{U}\sum_{m=1}^{M_t}\sum_{n=1}^{N_r}\mu_{jmn}+1;\ \frac{1}{1+2\lambda_{111}^x},\ \frac{1}{1+2\lambda_{112}^x},\ \ldots,\ \frac{1}{1+2\lambda_{UM_tN_r}^x},\ \frac{1}{1+2\lambda_{111}^y},\ \frac{1}{1+2\lambda_{112}^y},\ \ldots,\ \frac{1}{1+2\lambda_{UM_tN_r}^y}\right) \tag{18}$$

$$I_1 = \frac{\Gamma(2N_rM_tU\mu+0.5)}{2\sqrt{\pi}\Gamma(2N_rM_tU\mu+1)}(1+2g_{\mathrm{MPSK}}\lambda_1^x)^{-\mu(N_rM_tU-1)}(1+2g_{\mathrm{MPSK}}\lambda_1^y)^{-\mu(N_rM_tU-1)}(1+2g_{\mathrm{MPSK}}\lambda_2^x)^{-\mu} \times (1+2g_{\mathrm{MPSK}}\lambda_2^y)^{-\mu}F_D^4\left(0.5,\ \mu(N_rM_tU-1),\ \mu(N_rM_tU-1),\ \mu,\ \mu;2N_rM_tU\mu+1;\ \frac{1}{1+2g_{\mathrm{MPSK}}\lambda_1^x},\ \frac{1}{1+2g_{\mathrm{MPSK}}\lambda_1^y},\ \frac{1}{1+2g_{\mathrm{MPSK}}\lambda_2^x},\ \frac{1}{1+2g_{\mathrm{MPSK}}\lambda_2^y}\right) \tag{21}$$

$$I_2 = (1+2g_{\mathrm{MPSK}}\lambda_1^x)^{-\mu(N_rM_tU-1)}(1+2g_{\mathrm{MPSK}}\lambda_1^y)^{-\mu(N_rM_tU-1)}(1+2g_{\mathrm{MPSK}}\lambda_2^x)^{-\mu}(1+2g_{\mathrm{MPSK}}\lambda_2^y)^{-\mu} \times F_D^5\left(0.5,\ 0.5-2N_rM_tU\mu,\ \mu(N_rM_tU-1),\ \mu(N_rM_tU-1),\ \mu,\ \mu;\ 1.5;\ \cos^2\frac{\pi}{M},\ \frac{\cos^2(\pi/M)}{1+2g_{\mathrm{MPSK}}\lambda_1^x},\ \frac{\cos^2(\pi/M)}{1+2g_{\mathrm{MPSK}}\lambda_1^y},\ \frac{\cos^2(\pi/M)}{1+2g_{\mathrm{MPSK}}\lambda_2^x},\ \frac{\cos^2(\pi/M)}{1+2g_{\mathrm{MPSK}}\lambda_2^y}\right) \tag{22}$$

distribution is another special case of η–μ fading distribution then, putting $U=1$, $K=1$, $M_t=1$ and $N_r=L$, (24) and (25) collapse to [25, Eq. (7)].

4.3 ASEP of square MQAM digital modulation technique

In this case, we compute the ASEP of square MQAM digital modulation for MIMO MC DS CDMA system functioning over arbitrarily and equally correlated η–μ fading channels. The conditional error probability of the MQAM is as given in [20] and its alternative representation is given by [21]

$$P_{\mathrm{MQAM}} = \frac{4q}{\pi}\int_0^{0.5\pi} \exp\left(-\frac{\gamma g_{\mathrm{MQAM}}}{\sin^2\theta}\right)\mathrm{d}\theta - \frac{4q^2}{\pi}\int_0^{0.25\pi} \exp\left(-\frac{\gamma g_{\mathrm{MQAM}}}{\sin^2\theta}\right)\mathrm{d}\theta \tag{26}$$

where $q=1-M^{-0.5}$ and $g_{\mathrm{MQAM}}=1.5(M-1)^{-1}$. Therefore the ASEP of square MQAM digital modulation format using (12) is

$$P_{s,\mathrm{MQAM}} = \frac{4q}{\pi}\int_0^{0.5\pi} \Phi_{x+y}\left(\frac{g_{\mathrm{MQAM}}}{\sin^2\theta}\right)\mathrm{d}\theta - \frac{4q^2}{\pi}\int_0^{0.25\pi} \Phi_{x+y}\left(\frac{g_{\mathrm{MQAM}}}{\sin^2\theta}\right)\mathrm{d}\theta \tag{27}$$

Hence, employing the substitution $t=\cos^2\theta$ to the first integral and simplify, we have (see (28))

The second integral can be obtained by utilising the substitution $t=1-\tan^2\theta$, then simplifying further, we have (see (29) on the bottom of the next page)

Finally, the difference between I_1 and I_2 produces the ASEP of square MQAM digital modulation scheme for the system operating over equally correlated η–μ fading channels.

In addition, we can derive the ASEP of square MQAM digital modulation technique for MIMO MC DS CDMA system working over arbitrarily correlated η–μ fading channels using (13) and (26), hence (see (30) on the bottom of the next page)

$$P_{S,\mathrm{MPSK}} = \frac{1}{\pi}\int_0^{0.5\pi}\prod_{j=1}^{U}\prod_{m=1}^{M_t}\prod_{n=1}^{N_t}\left(1+\frac{2g_{\mathrm{MPSK}}\lambda_{jmn}^{x}}{\sin^2\theta}\right)^{-\mu_{jmn}}\left(1+\frac{2g_{\mathrm{MPSK}}\lambda_{jmn}^{y}}{\sin^2\theta}\right)^{-\mu_{jmn}}\mathrm{d}\theta + \frac{1}{\pi}\int_{0.5\pi}^{\pi(1-M^{-1})}\prod_{j=1}^{U}\prod_{m=1}^{M_t}\prod_{n=1}^{N_r}\left(1+\frac{2g_{\mathrm{MPSK}}\lambda_{jmn}^{x}}{\sin^2\theta}\right)^{-\mu_{jmn}}\left(1+\frac{2g_{\mathrm{MPSK}}\lambda_{jmn}^{y}}{\sin^2\theta}\right)^{-\mu_{jmn}}\mathrm{d}\theta \tag{23}$$

$$I_1 = \frac{\Gamma\left(2\sum_{j=1}^{U}\sum_{m=1}^{M_t}\sum_{n=1}^{N_r}\mu_{jmn}+0.5\right)}{2\sqrt{\pi}\,\Gamma\left(2\sum_{j=1}^{U}\sum_{m=1}^{M_t}\sum_{n=1}^{N_r}\mu_{jmn}+1\right)}\left(\prod_{j=1}^{U}\prod_{m=1}^{M_t}\prod_{n=1}^{N_r}(1+2g_{\mathrm{MPSK}}\lambda_{jmn}^{x})^{-\mu_{jmn}}(1+2g_{\mathrm{MPSK}}\lambda_{jmn}^{y})^{-\mu_{jmn}}\right) \times F_D^{(2UM_tN_r)}\left(0.5,\ \mu_{111},\ \mu_{112},\ \ldots,\ \mu_{UM_tN_r},\ \mu_{111},\ \mu_{112},\ \ldots,\ \mu_{UM_tN_r};\ 2\sum_{j=1}^{U}\sum_{m=1}^{M_t}\sum_{n=1}^{N_r}\mu_{jmn}+1;\ \frac{1}{1+2g_{\mathrm{MPSK}}\lambda_{111}^{x}},\ \frac{1}{1+2g_{\mathrm{MPSK}}\lambda_{112}^{x}},\ \ldots,\ \frac{1}{1+2g_{\mathrm{MPSK}}\lambda_{UM_tN_r}^{x}},\ \frac{1}{1+2g_{\mathrm{MPSK}}\lambda_{111}^{y}},\ \frac{1}{1+2g_{\mathrm{MPSK}}\lambda_{112}^{y}},\ \ldots,\ \frac{1}{1+2g_{\mathrm{MPSK}}\lambda_{UM_tN_r}^{y}}\right) \tag{24}$$

$$I_2 = \frac{\cos(\pi/M)}{\pi}\left(\prod_{j=1}^{U}\prod_{m=1}^{M_t}\prod_{n=1}^{N_r}(1+2g_{\mathrm{MPSK}}\lambda_{jmn}^{x})^{-\mu_{jmn}}(1+2g_{\mathrm{MPSK}}\lambda_{jmn}^{y})^{-\mu_{jmn}}\right) \times F_D^{(2UM_tN_r+1)}\left(0.5,\ 0.5-2\sum_{j=1}^{U}\sum_{m=1}^{M_t}\sum_{n=1}^{N_r}\mu_{jmn},\ \mu_{111},\ \mu_{112},\ \ldots,\ \mu_{UM_tN_r},\ \mu_{111},\ \mu_{112},\ \ldots,\ \mu_{UM_tN_r};\ 1.5;\ \cos^2(\pi/M),\ \frac{\cos^2(\pi/M)}{1+2g_{\mathrm{MPSK}}\lambda_{111}^{x}},\ \frac{\cos^2(\pi/M)}{1+2g_{\mathrm{MPSK}}\lambda_{112}^{x}},\ \ldots,\ \frac{\cos^2(\pi/M)}{1+2g_{\mathrm{MPSK}}\lambda_{111}^{y}},\ \frac{\cos^2(\pi/M)}{1+2g_{\mathrm{MPSK}}\lambda_{112}^{y}},\ \ldots,\ \frac{\cos^2(\pi/M)}{1+2g_{\mathrm{MPSK}}\lambda_{UM_tN_r}^{y}}\right) \tag{25}$$

$$I_1 = \frac{2q\Gamma(2N_rM_tU\mu+0.5)}{\sqrt{\pi}\Gamma(2N_rM_tU\mu+1)}(1+2\lambda_1^{x}g_{\mathrm{MQAM}})^{-\mu(N_rM_tU-1)}(1+2\lambda_1^{y}g_{\mathrm{MQAM}})^{-\mu(N_rM_tU-1)}(1+2\lambda_2^{x}g_{\mathrm{MQAM}})^{-\mu} \times (1+2\lambda_2^{y}g_{\mathrm{MQAM}})^{-\mu}F_D^{4}\left(0.5,\ \mu(N_rM_tU-1),\ \mu(N_rM_tU-1),\ \mu,\ \mu;\ 2N_rM_tU\mu+1;\ \frac{1}{1+2\lambda_1^{x}g_{\mathrm{MQAM}}},\ \frac{1}{1+2\lambda_1^{y}g_{\mathrm{MQAM}}},\ \frac{1}{1+2\lambda_2^{x}g_{\mathrm{MQAM}}},\ \frac{1}{1+2\lambda_2^{y}g_{\mathrm{MQAM}}}\right) \tag{28}$$

doi: 10.1049/iet-com.2014.0046

Considering the first integral, put $t = \cos^2\theta$, use basic ideas of calculus and algebra, we have (see (31))

Similarly, put $t = 1–\tan^2\theta$ in the second part of (30) and then making necessary manipulations, we have (see (32))

Therefore the difference between I_1 and I_2 yields the ASEP of square MQAM modulation scheme for MIMO MC DS CDMA system over arbitrarily correlated η–μ fading channels. Since η–μ fading distribution can diminish to Nakagami-q ($\mu = 0.5$, $b = (1-\eta)/(1+\eta)$, $q = \sqrt{\eta}$) distribution as a special case, then, suppose $U = 1$, $K = 1$ and the system operates in an i.i.d (correlation coefficient $r = 0$) η–μ fading environment, the difference between I_1 and I_2 collapses to [23, Eq. (13)]. Similarly, since Nakagami-m ($\eta \to 0$, $\eta \to \infty$, $\eta \to \pm 1$) distribution is a particular case of η–μ fading distribution, then (31) and (32) drop to [25, Eq. (12)].

5 Numerical examples and discussions

In this section, we present numerical results to illustrate the performance of the MC DS CDMA MIMO system operating over correlated η–μ fading channels in terms of average error probability. We investigate the effects of correlation coefficient and the number of multipath clusters on the system performance numerically. The parameters used for the analysis of the system are indicated in each graph. We employ infinite series representation of Lauricella's multivariate hypergeometric functions for average error probability of the system to write a code in MATLAB software package in order to generate the graphs presented below. In this case, the number of terms used for computation is 20. On the other hand, Monte Carlo simulation technique is used to validate the results obtained via analytical solution. Hence, the number of random variables generated is 10^5.

Fig. 1 shows graphically the effect of correlation on average bit error rate performance of multiple-input–single-output MC DS CDMA (MISO MC DS CDMA) system over correlated η–μ frequency non-selective fading channels. As expected, the ABEP of the system increase as the correlation coefficient ($r = 0.1,\ 0.3,\ 0.5$) increases. Similarly, it is confirmed that the performance of SISO MC DS CDMA system is inferior to that of MISO MC DS CDMA system. In Fig. 2, we illustrate graphically the

$$I_2 = \frac{q^2\Gamma(2N_rM_tU\mu + 0.5)}{\pi\Gamma(2N_rM_tU\mu + 1)}(1 + 4\lambda_1^x g_{MQAM})^{-\mu(N_rM_tU-1)}(1 + 4\lambda_1^y g_{MQAM})^{-\mu(N_rM_tU-1)}(1 + 4\lambda_2^x g_{MQAM})^{-\mu} \times \left(1 + 4\lambda_2^y g_{MQAM}\right)^{-\mu} F_D^5\left(1,\ 1,\ \mu(N_rM_tU-1),\ \mu(N_rM_tU-1),\ \mu,\ \mu;\ 2N_rM_tU\mu + 1.5;\ 0.5,\ \frac{1 + 2\lambda_1^x g_{MQAM}}{1 + 4\lambda_1^x g_{MQAM}},\ \frac{1 + 2\lambda_1^y g_{MQAM}}{1 + 4\lambda_1^y g_{MQAM}},\ \frac{1 + 2\lambda_2^x g_{MQAM}}{1 + 4\lambda_2^x g_{MQAM}},\ \frac{1 + 2\lambda_2^y g_{MQAM}}{1 + 4\lambda_2^y g_{MQAM}}\right) \tag{29}$$

$$P_{MQAM} = \frac{4q}{\pi}\int_0^{0.5\pi}\prod_{j=1}^{U}\prod_{m=1}^{M_t}\prod_{n=1}^{N_r}\left(1 + \frac{2g_{MQAM}\lambda_{jmn}^x}{\sin^2\theta}\right)^{-\mu_{jmn}}\left(1 + \frac{2g_{MQAM}\lambda_{jmn}^y}{\sin^2\theta}\right)^{-\mu_{jmn}} d\theta - \frac{4q^2}{\pi}\int_0^{0.25\pi}\prod_{j=1}^{U}\prod_{m=1}^{M_t}\prod_{n=1}^{N_r}\left(1 + \frac{2g_{MQAM}\lambda_{jmn}^x}{\sin^2\theta}\right)^{-\mu_{jmn}}\left(1 + \frac{2g_{MQAM}\lambda_{jmn}^y}{\sin^2\theta}\right)^{-\mu_{jmn}} d\theta \tag{30}$$

$$I_1 = \frac{2q\Gamma\left(2\sum_{j=1}^{U}\sum_{m=1}^{M_t}\sum_{n=1}^{N_r}\mu_{jmn} + 0.5\right)}{\sqrt{\pi}\Gamma\left(2\sum_{j=1}^{U}\sum_{m=1}^{M_t}\sum_{n=1}^{N_r}\mu_{jmn} + 1\right)}\left(\prod_{j=1}^{U}\prod_{m=1}^{M_t}\prod_{n=1}^{N_r}(1 + 2g_{MQAM}\lambda_{jmn}^x)^{-\mu_{jmn}}(1 + 2g_{MQAM}\lambda_{jmn}^y)^{-\mu_{jmn}}\right) \times F_D^{(2UM_tN_r)}\left(0.5,\ \mu_{111},\ \mu_{112},\ \ldots,\ \mu_{UM_tN_r},\ \mu_{111},\ \mu_{112},\ \ldots,\ \mu_{UM_tN_r};\ 2\sum_{j=1}^{U}\sum_{m=1}^{M_t}\sum_{n=1}^{N_r}\mu_{jmn} + 1;\ \frac{1}{1 + 2g_{MQAM}\lambda_{111}^x},\ \frac{1}{1 + 2g_{MQAM}\lambda_{112}^x},\ \ldots,\ \frac{1}{1 + 2g_{MQAM}\lambda_{UM_tN_r}^x},\ \frac{1}{1 + 2g_{MQAM}\lambda_{111}^y},\ \frac{1}{1 + 2g_{MQAM}\lambda_{112}^y},\ \ldots,\ \frac{1}{1 + 2g_{MQAM}\lambda_{UM_tN_r}^y}\right) \tag{31}$$

$$I_2 = \frac{q\Gamma\left(2\sum_{j=1}^{U}\sum_{m=1}^{M_t}\sum_{n=1}^{N_r}\mu_{jmn} + 0.5\right)}{\pi\Gamma\left(2\sum_{j=1}^{U}\sum_{m=1}^{M_t}\sum_{n=1}^{N_r}\mu_{jmn} + 1.5\right)}\left(\prod_{j=1}^{U}\prod_{m=1}^{M_t}\prod_{n=1}^{N_r}(1 + 4g_{MQAM}\lambda_{jmn}^x)^{-\mu_{jmn}}(1 + 4g_{MQAM}\lambda_{jmn}^y)^{-\mu_{jmn}}\right) \times F_D^{(2UM_tN_r+1)}\left(1,\ 1,\ \mu_{111},\ \mu_{112},\ \ldots,\ \mu_{UM_tN_r},\ \mu_{111},\ \mu_{112},\ \ldots,\ \mu_{UM_tN_r};\ 2\sum_{j=1}^{U}\sum_{m=1}^{M_t}\sum_{n=1}^{N_r}\mu_{jmn} + 1.5;\ 0.5,\ \frac{1 + 2g_{MQAM}\lambda_{111}^x}{1 + 4g_{MQAM}\lambda_{111}^x},\ \frac{1 + 2g_{MQAM}\lambda_{112}^x}{1 + 4g_{MQAM}\lambda_{112}^x},\ \ldots,\ \frac{1 + 2g_{MQAM}\lambda_{UM_tN_r}^x}{1 + 4g_{MQAM}\lambda_{UM_tN_r}^x},\ \frac{1 + 2g_{MQAM}\lambda_{111}^y}{1 + 4g_{MQAM}\lambda_{111}^y},\ \frac{1 + 2g_{MQAM}\lambda_{112}^y}{1 + 4g_{MQAM}\lambda_{112}^y},\ \ldots,\ \frac{1 + 2g_{MQAM}\lambda_{UM_tN_r}^y}{1 + 4g_{MQAM}\lambda_{UM_tN_r}^y}\right) \tag{32}$$

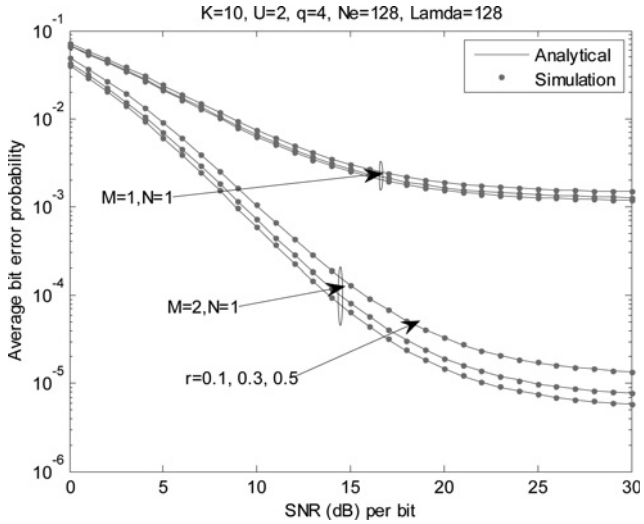

Fig. 1 *ABEP against average SNR of BPSK modulation technique for SISO and MISO MC DS CDMA system over correlated η–μ frequency non-selective fading channels (η = 1.5, and μ = 0.5: format 1 scenario)*

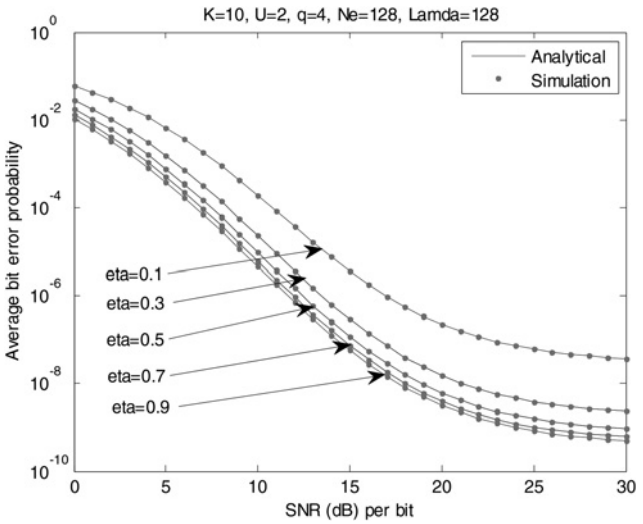

Fig. 3 *Effect of η on ABEP of BPSK modulation technique for MIMO MC DS CDMA system operating over correlated η–μ frequency non-selective fading channels (μ = 0.5, ρ = 0.3, M_t = 2 and N_r = 2: format 1 scenario)*

influence of correlation coefficient on average bit error rate performance for single-input–multiple-output MC DS CDMA (SIMO MC DS CDMA) system operating over correlated η–μ flat fading channels. Hence, as the correlation coefficient ($r = 0.1$, 0.3, 0.5) increases, the ABEP increases as well. Therefore the system performance deteriorates. On the other hand, it is observed that the performance of SIMO MC DS CDMA system operating over correlated η–μ frequency non-selective fading channels outperforms that of MISO MC DS CDMA system transmitting over the same channels. Since it is assumed that the transmit power employed for both cases (single-input–multiple-output, SIMO and multiple-input–single-output, MISO) is the same, say P, then in case of M_t transmit antennas, each antenna will radiate P/M_t power for transmission in order to confirm the same total radiated power as with one transmit antenna. In this case, fading is severe. However, for the case of single transmit antenna with P transmit power and many receive antennas, the prospect of receiving signals not all in deep fade is possible. Therefore the performance of MISO system is lower than that of SIMO system over the same fading channel. Fig. 3 exemplifies the influence of η parameter on ABEP in format 1 scenario. In this case, as η increases, the ABEP decreases and the system performance improves. This is because of the increase in power ratio between the in-phase signal component and the quadrature signal component of each cluster of multipath. Suppose K (user) = 1, U (subcarrier) = 1, $M_t = 1$, $N_r = 1$ and the correlation coefficient is zero, the results reduced to that in [16, 26]. In Fig. 4, the effect of η fading parameter on ABER system performance is depicted graphically. Hence, as η increases, the ABEP of BPSK modulation technique for the system increases as well. The main reason behind this is that the

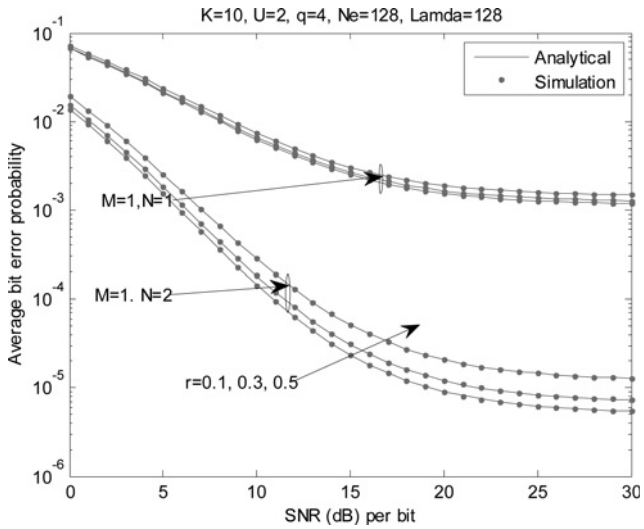

Fig. 2 *ABEP against average SNR of BPSK modulation scheme for SISO and SIMO MC DS CDMA system transmitting over correlated η–μ flat fading channels (η = 1.5, and μ = 0.5: format 1 scenario)*

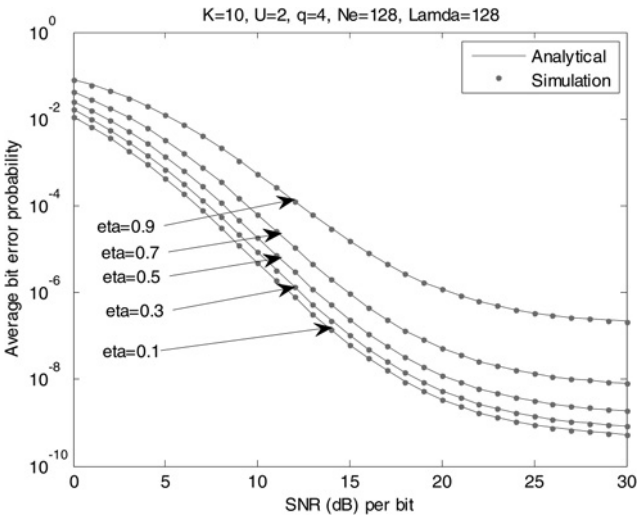

Fig. 4 *Impact of η fading parameter on ABEP of BPSK modulation scheme for MIMO MC DS CDMA system operating over correlated η–μ frequency non-selective fading channels (μ = 0.5, ρ = 0.3, M_t = 2 and N_r = 2: format 2 scenario)*

doi: 10.1049/iet-com.2014.0046

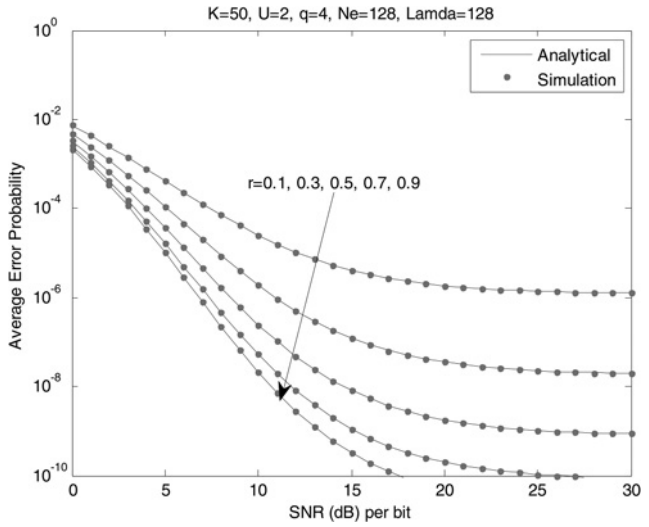

Fig. 5 *ABEP of BPSK modulation for MC DS CDMA MIMO system working over correlated η–μ fading channels ($M_t = 2$, $N_r = 2$, $U = 2$, $\eta = 1.5$ and $\mu = 3$: format 1 scenario)*

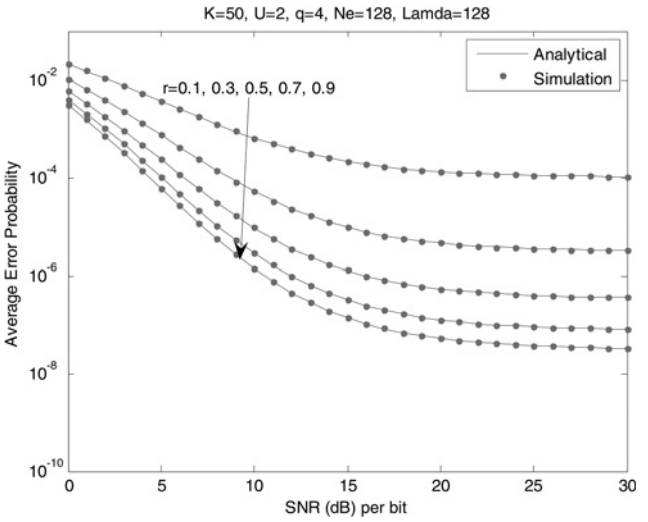

Fig. 7 *ABEP of BPSK for MC DS CDMA MIMO system operating over correlated η–μ fading channels ($M_t = 2$, $N_r = 2$, $U = 2$, $\eta = 2$ and $\mu = 1$: format 1 scenario)*

in-phase component and quadrature component of the transmitted signal are correlated. So if $K = 1$, $U = 1$, $M_t = 1$, $N_r = 1$ and the correlation coefficient is zero, these results drop to that in [26]. Generally, the physical phenomenon represented by the fading parameter η in format 1 scenario is absolutely distinct from that represented in format 2 scenario as shown in Figs. 3 and 4. Thus, Figs. 1–4 are derived from (17).

Based on (17), we generate the graph depicted in Fig. 5 with the parameters indicated. In this case, the values of the parameters employed are $K = 50$, $M_t = 2$, $N_r = 2$, $U = 2$, $\eta = 1.5$ and $\mu = 3$, respectively. The type of format used is format 1. Thus, the figure shows the results of the system operating over correlated η–μ fading channel in terms of ABEP of BPSK digital modulation technique against SNR per bit. The curves for the ABEP against SNR per bit vary because of the variation in correlation coefficients ($r = 0.1$, 0.3, 0.5, 0.7, 0.9), respectively. We observe as expected, the ABEP decreases as SNR per bit increases and increases because of the effect of correlation coefficient. Fig. 6 is also obtained from (17) and the parameters utilised are all shown. As a numerical example, the operation of the system over correlated η–μ fading channels is based on the following parameters $M_t = 2$, $N_r = 2$, $U = 2$, $\eta = 2$, $\mu = 1.5$ and $K = 50$ users and are specified at the top of the graph. Here, the plots for ABEP vary (increasingly) because of the following correlation coefficients $r = 0.1$, 0.3, 0.5, 0.7 and 0.9, respectively. It is obvious that, the ABEP increases in value compared with that in Fig. 5 owing to small number of multipath clusters employed in the environment. In addition, the system operation is simulated via Monte Carlo simulation method, as shown, the results agree well with that obtain using analytical method. Fig. 7 depicts the performance of the system over correlated η–μ fading environment in terms of ABEP. So the parameters used are as follows $M_t = 2$, $N_r = 2$, $U = 2$, $\eta = 2$ and $\mu = 1$ and are indicated at the top of the graph and inside. We observe that, the system performance deteriorates because of the small number of the multipath

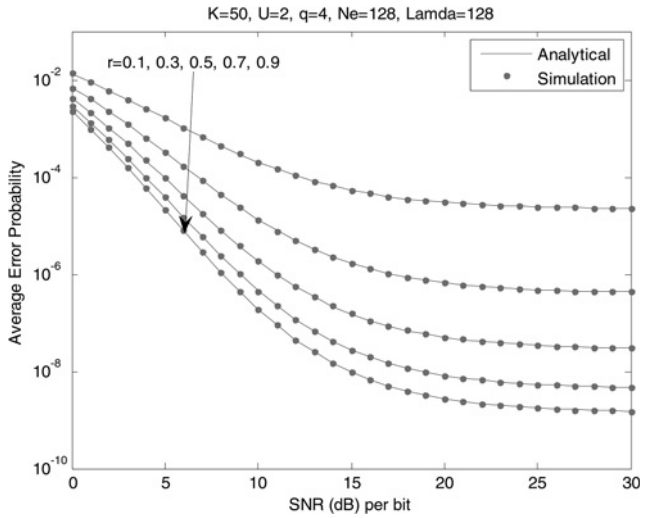

Fig. 6 *ABEP of BPSK for MC DS CDMA MIMO system functioning over correlated η–μ fading channels ($M_t = 2$, $N_r = 2$, $U = 2$, $\eta = 2$ and $\mu = 1.5$: format 1 scenario)*

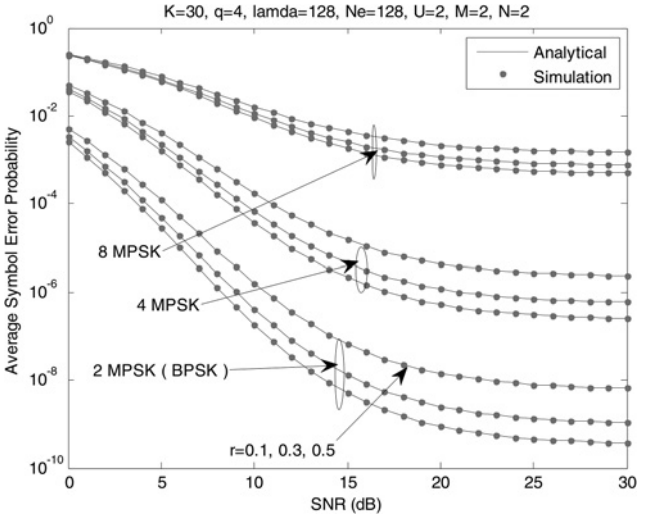

Fig. 8 *ASEP of 2, 4, 8 PSK for MC DS CDMA MIMO system working over correlated η–μ fading channels ($M_t = 2$, $N_r = 2$, $U = 2$, $K = 30$, $\eta = 2$ and $\mu = 1$: format 1 situation)*

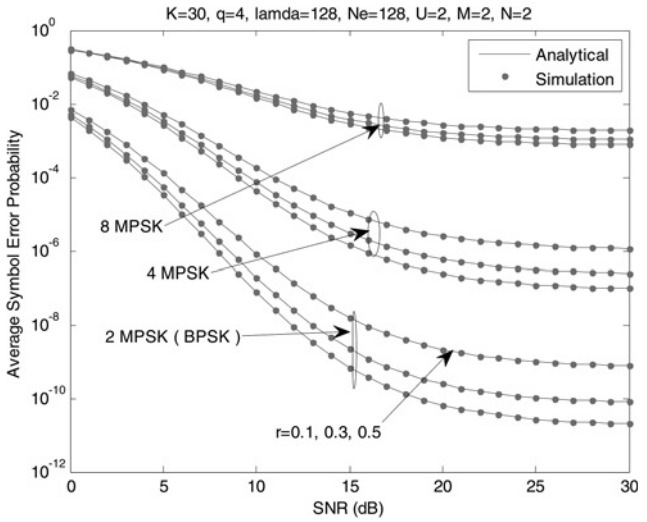

Fig. 9 *ASEP of 2, 4, 8 PSK for MC DS CDMA MIMO system operating over η–μ fading channels ($M_t = 2$, $N_r = 2$, $U = 2$, $K = 30$, $\eta = 1$ and $\mu = 1.5$: format 1 scenario)*

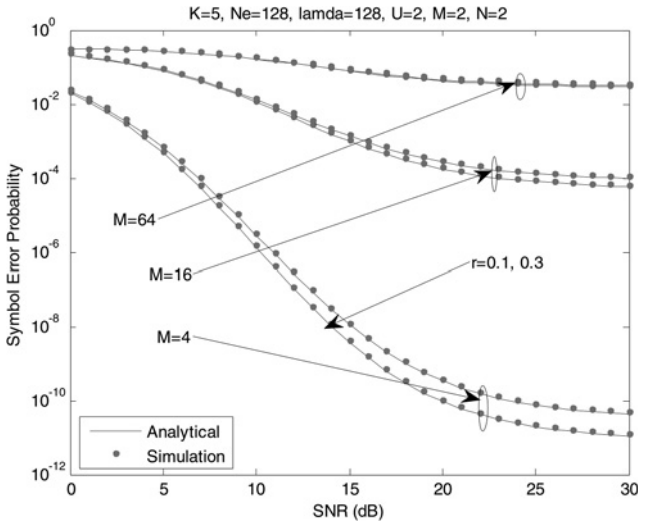

Fig. 11 *ASEP of 4, 16, 64 QAM for MC DS CDMA MIMO system operating over correlated η–μ fading channels ($M_t = 2$, $N_r = 2$, $U = 2$, $K = 5$ users, $\eta = 1.5$ and $\mu = 1.5$: format 1 scenario)*

clusters and the effect of correlation. We confirm the analytical technique using Monte Carlo simulation method and the results are in good agreement.

Fig. 8 exemplifies the ASEP of MPSK modulation scheme for MC DS CDMA MIMO system working over correlated η–μ fading channels using the following parameters $M = 2$, 4, 8, $M_t = 2$, $N_t = 2$, $U = 2$, $K = 30$ users, $\eta = 2$ and $\mu = 1$ for format 1. As shown, we note that the system performance degrades when the signal constellation size increases and also when the value of correlation coefficient between the signals spectra increases as the space between the receiving antennas decreases. Similarly, Fig. 9 demonstrates the results of the system operating over correlated η–μ fading environment based on the following parameters: $M_t = 2$, $N_r = 2$, $U = 2$, $K = 30$ users, $\eta = 1$ and $\mu = 1.5$ for format 1. In this case, we notice that the ASEP of the system decreases because of the increase in parameter μ. This, however, enhances the performance of the system over correlated η–μ fading channels. We verify the analytical method via Monte Carlo simulation technique. Hence, suppose $U = 1$, $K = 1$ and correlation coefficient ($r = 0$) is zero (i.i.d), then, the results in Figs. 8 and 9 reduce to that in [23].

Fig. 10 elucidates the operation of the system over correlated η–μ fading channels in terms of ASEP of square MQAM digital modulation scheme. Hence, the fading parameters employed are $\eta = 1.5$ and $\mu = 1.5$ for format 1 scenario. Analogously, the values of the correlation coefficient are indicated in the graph. The size of the signal constellation is $M = 4$. Therefore the value of the ASEP increases because of the effect of correlation coefficient. In this case, we authenticate the analytical solution via Monte Carlo simulation method. The performance of the system in correlated η–μ fading environment in terms of ASEP of square MQAM with variable signal constellation size ($M = 4$, 16, 64) is depicted in Fig. 11. The fading parameters utilised are as follows $\eta = 1.5$ and $\mu = 1.5$ for format 1 situation. As expected, we observe that the ASEP of the system increases because of the increase in signal constellation size as well as correlation coefficient. As illustrated in Fig. 11, we substantiate the analytical method through Monte Carlo simulation technique. In case of special cases, suppose $U = 1$, $K = 1$ and the correlation coefficient is zero ($r = 0$), the results in Figs. 10 and 11 drop to that in [23].

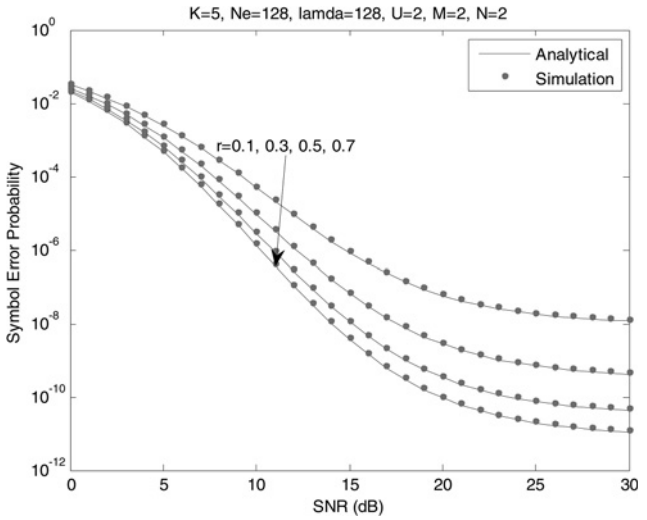

Fig. 10 *ASEP of 4QAM for MC DS CDMA MIMO system functioning over correlated η–μ fading channels ($M_t = 2$, $N_r = 2$, $U = 2$, $\eta = 1.5$ and $\mu = 1.5$: format 1 scenario)*

6 Conclusion

In this paper, the performance of MIMO MC DS CDMA system operating over correlated η–μ fading channels in terms of average error probability have been investigated. We derived exact closed form expressions for average error probability of coherent binary and M-ary digital modulation techniques for the system working over arbitrarily and equally correlated η–μ fading environment. The average error probability expressions are expressed in terms of Lauricella's multivariate hypergeometric functions which are easily manageable using software packages such as MATLAB. We observed that, deterioration in system performance was because of the effect of correlation and increase in size of the signal constellations. In case of signal constellation size, the performance of the system degrades because of the decreasing Euclidean distance

doi: 10.1049/iet-com.2014.0046

between the symbols for constant average signal energy (E_s). However, an acceptable space separation between two adjacent subcarriers and also increasing the number of subcarriers (frequency diversity) will improve the system performance. On the other hand, the influence of η fading parameter on average error probability of the system operating over correlated η–μ flat fading channels in format 1 scenario causes improvement in system performance as η increases and deterioration in system performance in format 2 as η increases. This is because in format 1 situation the increase in power ratio between the in-phase and quadrature components of the received signal of each cluster of the multipath contributes to the system performance enhancement while in format 2 scenario the in-phase and quadrature components are correlated. Furthermore, we noticed that increasing the number of multipath clusters (μ) reduces the detrimental effect of fading and enhances the performance of the system. We validated our results via Monte Carlo simulation-based approach and found to agree well. In addition, we simplified η–μ fading distribution to its particular cases such as Nakagami-q and Nakagami-m distributions, respectively. Generally, as expected, we observed that the performance of MIMO MC DS CDMA system over correlated η–μ frequency non-selective fading channels is superior to that of SISO, MISO and SIMO MC DS CDMA systems transmitting over the same channels.

7 Acknowledgments

The authors would like to thank and recognise PETRONAS for financial support. Furthermore, the authors would like to extend their thankfulness to the anonymous reviewers for constructive suggestions which leads to the substantial improvement of the paper. The authors also express gratitude to Dr. Shen for his valuable comments that further enhances this paper.

8 References

1 Yang, L.L.: 'Multicarrier communications' (John Wiley & Sons, 2009)
2 Hara, S., Prasad, R.: 'Overview of multicarrier CDMA', *IEEE Commun. Mag.*, 1997, **35**, (12), pp. 126–132
3 Li, Z., Latva-aho, M.: 'Error probability of interleaved MC CDMA system with MRC receiver and correlated Nakagami-*m* fading channels', *IEEE Trans. Commun.*, 2005, **53**, (6), pp. 919–923
4 Feng, Y., Qin, J.: 'BER of MC CDMA systems with MRC in correlated Nakagami-*m* fading', *IEEE Electron. Lett.*, 2005, **41**, (19), pp. 1069–1071
5 Feng, Y., Qin, J.: 'BER of MC CDMA systems with EGC in correlated Nakagami-*m* fading', *IEEE Commun. Lett.*, 2006, **10**, (10), pp. 689–691
6 Yao, G.X., Liu, Z.W., Xu, Y.G., Gong, X.F.: 'Antenna selection in space time block coded MC CDMA systems'. Proc. Int. Conf. on Signal Processing, 2006, pp. 16–20
7 Xu, W., Milstein, L.B.: 'On the performance of multicarrier RAKE systems', *IEEE Trans. Commun.*, 2001, **49**, (10), pp. 1812–1823
8 Elnoubi, S.M., Hashem, A.A.: 'Error rate performance of MC DS CDMA systems over multiple input multiple output Nakagami-*m* fading channel'. Proc. Military Commun. Conf., San Diego, CA, 2008
9 Lodhi, A., Said, F., Dohler, M., Aghvami, H.: 'Closed-form symbol error probability of STBC and CDD MC-CDMA with frequency-correlated subcarriers over Nakagami-*m* fading channels', *IEEE Trans. Veh. Technol.*, 2008, **57**, (2), pp. 962–973
10 Yang, L.-L.: 'Performance of multiantenna multicarrier direct-sequence code division multiple access using orthogonal variable spreading factor codes-assisted space–time spreading in time selective fading channels', *IET Commun.*, 2008, **2**, (5), pp. 708–719
11 Shaban, H., El-Nasr, M.A., Buehre, R.M.: 'BER Performance of MRC/MC-CDMA systems for MSK scheme in independent and correlated Nakagami-*m* and Rician fading channels'. IEEE Int. Symp. on Proc. Signal Processing and Information Technology, 2009, 14–17 December 2009, pp. 15–19
12 Asghari, V., Costa, D.B.da, Aissa, S.: 'Symbol error probability of rectangular QAM in MRC systems with correlated η-μ fading channels', *IEEE Trans. Veh. Technol.*, 2010, **59**, (3), pp. 1497–1503
13 Sabadar, R., Shu, P.R.: 'Performance of a L-MRC receiver fading channels', *IEEE Trans. Wirel. Commun.*, 2011, **10**, (5), pp. 1351–1355
14 Mark, J.O., Samir, B.B., Saad, N.M.: 'Capacity and error probability performance analysis for MIMO MC DS CDMA System in η-μ Fading Environment', *Int. J. Electron. Commun.*, 2013, **67**, pp. 269–281
15 Yacoub, M.D.: 'The κ-μ distribution and the η-μ distribution', *IEEE Antennas Propag. Mag.*, 2007, **49**, (1), pp. 68–81
16 Costa, D.B.da, Yacoub, M.D.: 'Moment generating functions of generalized fading distributions and applications', *IEEE Commun. Lett.*, 2008, **12**, (2), pp. 112–114
17 Alamouti, S.M.: 'A simple transmitter diversity scheme for wireless communication', *IEEE J. Sel. Areas Commun.*, 1998, **16**, (8), pp. 1451–1458
18 Alouini, M.-S., Abdi, A., Keveh, M.: 'Sum of gamma variates and performance of wireless communication systems over Nakagami-fading channels', *IEEE Trans. Veh. Techno.*, 2001, **50**, (6), pp. 1471–1480
19 Lombardo, P., Fedele, G., Rao, M.M.: 'MRC performance for binary signals in Nakagami fading with general branch correlation', *IEEE Trans. Commun.*, 1999, **47**, (1), pp. 44–52
20 Proakis, J.G.: 'Digital communications' (McGraw-Hill, New York, 2001, 4th edn.)
21 Craig, J.W.: 'A new, simple and exact results for calculating the probability of error for two dimensional signal constellations'. Proc. IEEE Military Commun. Conf. Mclean, VA, October 1991, pp. 571–575
22 Shin, H., Lee, J.H.: 'On error probability of binary and M-ary signals in Nakagami-*m* fading channels', *IEEE Trans. Commun.*, 2004, **52**, (4), pp. 536–539
23 Xu, F., Yue, D.-W., Zhou, Q.F.: 'Performance analysis of orthogonal space-time block codes over nakagami-*q* (Hoyt) fading channels'. Proc. IEEE Int. Conf. on Commun., May 2008, pp. 3966–3970
24 Peppas, K., Lazarakis, F., Alexandridis, A., Dangakis, K.: 'Error performance of digital modulation schemes with MRC diversity reception over η-μ fading channels', *IEEE Trans. Wirel. Commun.*, 2009, **8**, (10), pp. 4974–4980
25 Efthymoglou, G.P., Piboongungon, T., Aalo, V.A.: 'Error rates of *M*-ary signals with multichannel reception in Nakagami-*m* fading channels', *IEEE Commun. Lett.*, 2006, **10**, (2), pp. 100–102
26 Ermolova, N.Y.: 'Moment generating function of generalised η-μ and κ-μ distributions and their applications to performance evaluation s of communication systems', *IEEE Commun. Lett.*, 2008, **12**, (7), pp. 502–504
27 Li, W., Zhang, H., Gulliver, T.A.: 'Capacity and error probability analysis of orthogonal space-time block codes over correlated Nakagami fading channels', *IEEE Trans. Wirel. Commun.*, 2006, **5**, (9), pp. 2408–2412
28 Win, M.Z., Chrisikos, G., Winters, J.H.: 'MRC performance for M-ary modulation in arbitrarily correlated Nakagami fading channels', *IEEE Commun. Lett.*, 2000, **4**, (10), pp. 301–303
29 Miller, S.L., Childers, D.G.: 'Probability and random processes' (Academic Press, 2012, 2nd edn.)
30 Pierce, J.N., Stein, S.: 'Multiple diversity with nonindependent fading'. Proc. Proc. of the IRE, January 1960, pp. 89–104
31 Ermolova, N.Y.: 'Useful integrals for performance evaluation of communication systems in generalised η-μ and κ-μ fading channels', *IET Commun.*, 2009, **3**, (2), pp. 303–308

9 Appendix

9.1 Appendix 1

In this appendix, we derive the MGF of the instantaneous SINR at the output of the receiver. The envelope (R_{nm}) of the fading signal models η–μ fading distribution. Then, the random variable $\gamma = \left\| R_{nm}^2 \right\|$ has the PDF of η–μ distribution. Hence, a set of NMU variates of η–μ random variables is equivalent to a set of 2 μ independent Gaussian random variable vectors with NMU dimensions. Since the instantaneous SINR is given as [27]

$$\gamma_s = \gamma_c \sum_{n=1}^{N_t} \sum_{m=1}^{M_t} \sum_{j=1}^{U} \sum_{l=1}^{2\mu} R_{nmjl}^2 \tag{33}$$

where $R^2_{nmjl} = R^T_{nmjl}R_{nmjl} = X^T_{nmjl}X_{nmjl} + Y^T_{nmjl}Y_{nmjl}$, $X_{i=nmj} = [X_{i1}, X_{i2}, \ldots, X_{i2\mu}]^{\mathrm{T}}$ where $i = nmj = 1, 2, \ldots, N_rM_tU$ represents dependent in-phase random variables. Hence, X_{ik} are independent and identically distributed Gaussian random variables with zero mean and variance $E[X^2_{ik}]$, $k = 1, 2, \ldots, 2\mu$. Similarly, $Y_{i=nmj} = [Y_{i1}, Y_{i2}, \ldots, Y_{i2\mu}]^{\mathrm{T}}$ denote dependent quadrature random variables. Therefore, Y_{ik} are i.i.d Gaussian random variables with zero mean and variance $E[Y^2_{ik}]$ [28]. Both are mutually independent Gaussian variables with $E[X_{nmjl}] = E[Y_{nmjl}] = 0$, $E[X^2_{nmjl}] = \rho^2_x$, $E[Y^2_{nmjl}] = \rho^2_y$, μ is the number of clusters of multipath. Therefore the instantaneous SINR can be rewritten as

$$\gamma_s = \gamma_c \sum_{n=1}^{N_r}\sum_{m=1}^{M_t}\sum_{j=1}^{U}\sum_{l=1}^{2\mu} X^2_{nmjl} + \gamma_c \sum_{n=1}^{N_r}\sum_{m=1}^{M_t}\sum_{j=1}^{U}\sum_{l=1}^{2\mu} Y^2_{nmjl} \tag{34}$$

Considering the in-phase random variates $X^T_{ik}X_{ik}$, similarly, for quadrature random variates $Y^T_{ik}Y_{ik}$. For the case of in-phase random variates, we assume the arbitrary covariance matrix as $\boldsymbol{C_{xx}}$, then we can form a scalar quadratic function of vector $\boldsymbol{X}$, that is, suppose $Z = X^T_{nml}B_{nml}\boldsymbol{X}_{nml}$, where B_{nml} is a 2μ by 2μ matrix. Hence, the joint PDF of $\left[X^2_{nml1} + X^2_{nml2} + \cdots + X^2_{nml2\mu}\right]$ is [29]

$$f(X_{nml}) = \frac{1}{\sqrt{(2\pi)^{2\mu}\det(C_{xx})}}\exp\left(-\frac{1}{2}X^T_{nml}C^{-1}_{nml}X_{nml}\right) \tag{35}$$

Then, the MGF of Z is [29, 30] (see (36))

where **det** denotes determinant. Therefore, for NMU diversity branches, we have

$$\Phi_x(s) = \prod_{n=1}^{N_r}\prod_{m=1}^{M_t}\prod_{l=1}^{U}\frac{1}{\det(I_{nml} + 2sB_{nml}C^{nml}_{xx})^{\mu_{nml}}} \tag{37}$$

Similarly, for Y_{nml} (quadrature Gaussian variates), we have

$$\Phi_y(s) = \prod_{n=1}^{N_r}\prod_{m=1}^{M_t}\prod_{l=1}^{U}\frac{1}{\det(I_{nml} + s2B_{nml}D^{nml}_{yy})^{\mu_{nml}}} \tag{38}$$

where $\boldsymbol{D_{yy}}$ is the matrix. Therefore overall MGF of the instantaneous SINR at receiver output is (see (39))

9.2 Appendix 2

In this appendix, we employ Lauricella's multivariate hypergeometric function $F^n_D(.)$ to represent expressions for the average error probabilities of the system operating over η–μ fading channels. The Lauricella multivariate hypergeometric function is defined as [25, 31] (see (40))

where $\Gamma(a+i)/\Gamma(a)$ is a pochhammer symbol.

From (12) and (16), we have (see (41))

Use substitution $t = \cos^2\theta$ in (41), we have (see (42) at the bottom of the next page)

Hence, comparing (42) with (40), we have $a = 0.5$, $c = 2M_tN_rU\mu + 1$, $b_1 = \mu(M_tN_rU - 1)$, $b_2 = \mu(M_tN_rU - 1)$, $b_3 = \mu$ and $b_4 = \mu$, $x_1 = 1/(1 + 2\lambda^x_1)$, $x_2 = 1/(1 + 2\lambda^y_1)$, $x_3 = 1/(1 + 2\lambda^x_2)$, $x_4 = 1/(1 + 2\lambda^y_2)$. Therefore (17) is obtained. Furthermore, the subsequent equations can be derived in a similar approach.

$$\begin{aligned}\Phi_x(s) = E\left[\mathrm{e}^{-sX^T_{nml}B_{nml}X_{nml}}\right] &= \int_0^\infty \frac{1}{\sqrt{(2\pi)^{2\mu}\det(C_{xx})}}\mathrm{e}^{-(1/2)\left(X^T_{nml}(C^{-1}_{xx}+2sB_{nml})X_{nml}\right)}\mathrm{d}X_{nml}\\ &= \frac{\sqrt{\left(\det(F^{-1})\right)}}{\sqrt{\left(\det(C_{xx})\right)}}\int_0^\infty \frac{1}{\sqrt{(2\pi)^{2\mu}\left(\det(F)\right)}}\mathrm{e}^{-(1/2)X^TF^{-1}X}\,\mathrm{d}X = \frac{1}{\det(I_{nml} + 2sB_{nml}Cxx)^{\mu}}\end{aligned} \tag{36}$$

$$\Phi_{x+y}(s) = \prod_{n=1}^{N_r}\prod_{m=1}^{M_t}\prod_{l=1}^{U}\left(\frac{1}{\det(I_{nml} + 2sA_{nml}C^{nml}_{xx})^{\mu_{nml}}\det(I_{nml} + 2sB_{nml}D^{nml}_{yy})^{\mu_{nml}}}\right) \tag{39}$$

$$\begin{aligned}F^n_D(a, b_1, b_2, \ldots, b_n; c; x_1, x_2, \ldots, x_n) &= \frac{\Gamma(c)}{\Gamma(a)\Gamma(c-a)}\int_0^1 t^{a-1}(1-t)^{c-a-1}\prod_{i=1}^{n}(1-x_it)^{-b_i}\,\mathrm{d}t, \quad \mathrm{Re}(c-a) > 0, \quad \mathrm{Re}(a) > 0\\ &= \sum_{i_1,i_2,i_3,\ldots,i_n.=0}^{\infty}\frac{(a)_{i_1+i_2+\cdots+i_n}(b_1)_{i_1}(b_2)_{i_2}\cdots(b_n)_{i_n}}{(c)_{i_1+i_2+\cdots+i_n}i_1!i_2!\ldots i_n!}x_1^{i_1}x_2^{i_2}\ldots x_n^{i_n}\end{aligned} \tag{40}$$

$$P_b = \frac{1}{\pi}\int_0^{0.5\pi}\left(1 + \frac{2\lambda^x_1}{\sin^2\theta}\right)^{-\mu(M_tN_rU-1)}\left(1 + \frac{2\lambda^y_1}{\sin^2\theta}\right)^{-\mu(M_tN_rU-1)}\left(1 + \frac{2\lambda^x_2}{\sin^2\theta}\right)^{-\mu}\left(1 + \frac{2\lambda^y_2}{\sin^2\theta}\right)^{-\mu}\mathrm{d}\theta \tag{41}$$

doi: 10.1049/iet-com.2014.0046

$$P_b = \frac{1}{2\pi}(1+2\lambda_1^x)^{-\mu(M_tN_rU-1)}(1+2\lambda_1^y)^{-\mu(M_tN_rU-1)}(1+2\lambda_2^x)^{-\mu}(1+2\lambda_2^y)^{-\mu} \times \int_0^1 t^{-0.5}(1-t)^{2M_tN_rU\mu-0.5}\left(1-\frac{1}{1+2\lambda_1^x}t\right)^{-\mu(M_tN_rU-1)}\left(1-\frac{1}{1+2\lambda_1^y}t\right)^{-\mu(M_tN_rU-1)}\left(1-\frac{1}{1+2\lambda_2^x}t\right)^{-\mu}\left(1-\frac{1}{1+2\lambda_2^y}t\right)^{-\mu}\mathrm{d}t \quad (42)$$